Modification of a Designed Amphipathic Cell-Penetrating Peptide and Its Effect on Solubility, Secondary Structure, and Uptake Efficiency

ARTICLE *in* BIOCHEMISTRY · APRIL 2013

Impact Factor: 3.02 · DOI: 10.1021/bi4001326 · Source: PubMed

4 AUTHORS, INCLUDING:

Mousa Jafari
Massachusetts Institute of Technology
19 PUBLICATIONS **255** CITATIONS
SEE PROFILE

Nedra Karunaratne
University of Peradeniya
82 PUBLICATIONS **758** CITATIONS
SEE PROFILE

BIOCHEMISTRY
including biophysical chemistry & molecular biology

Article

pubs.acs.org/biochemistry

Modification of a Designed Amphipathic Cell-Penetrating Peptide and Its Effect on Solubility, Secondary Structure, and Uptake Efficiency

Mousa Jafari,[†,‡] D. Nedra Karunaratne,[†,§] Chad M. Sweeting,[†] and P. Chen*[,†,‡]

[†]Department of Chemical Engineering, and [‡]Waterloo Institute for Nanotechnology, University of Waterloo, Waterloo, Ontario N2L 3G1, Canada

[§]Department of Chemistry, University of Peradeniya, Peradeniya 20400, Sri Lanka

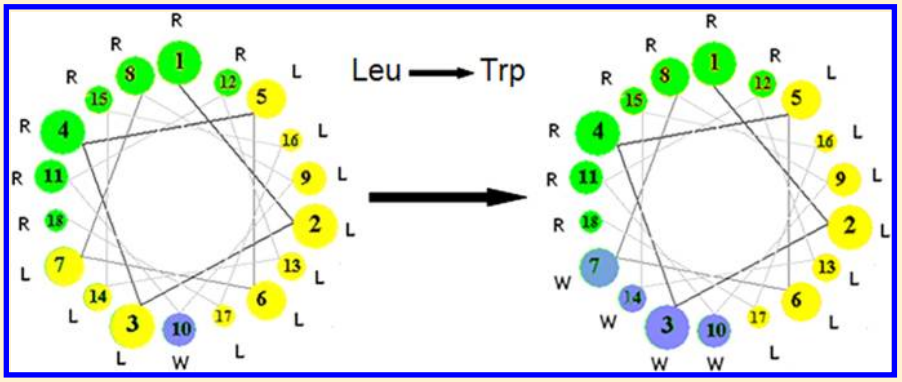

ABSTRACT: The development of safe and efficient nonviral gene delivery carriers has received a great deal of attention in the past decade. A class of amphipathic peptides has shown to be able to cross cell membranes and deliver cargo to the intracellular environment. Here, we introduce an 18-mer amphipathic peptide, C6M1, as a modified version of peptide C6 for short interfering RNA (siRNA) delivery. The importance of tryptophan residues and the effect of peptide sequence modification on its solubility, secondary structure, cytotoxicity, and uptake efficiency were investigated. The solubility of C6M1 in aqueous solutions was greatly enhanced compared to that of C6, confirmed by surface tension and anilinonaphthalene-8-sulfonic acid fluorescence measurements. C6M1 had a random/helical structure in water with the ability to attain a helical conformation in the presence of anionic components or membrane-mimicking environments. The modification significantly reduced the cytotoxicity of the peptide, making it a safer carrier for siRNA delivery. C6M1 was also found ~90% more efficient than C6 in delivering Cy3-labeled siRNA in Chinese hamster ovary cells.

With the ability of short interfering RNA (siRNA) to function as a therapeutic in gene therapy, efficient delivery and transfection of siRNA are of critical importance. The traditional nonviral carriers for gene therapy, such as liposomes and cationic polymers, are known to have more versatility than viral vectors. However, with the discovery that cell-penetrating peptides (CPPs) are able to cross biological membranes and deliver cargo into the intracellular matrix, an interest in peptides as carriers of nucleic acids has emerged. Peptide-based delivery systems have also shown the potential to deliver bioactive peptides, therapeutic proteins, and nucleic acids.[1−3] Their role is to deliver polypeptides and proteins into cells through either of two strategies: covalent or complexed in a non-covalent fashion.

Primary amphipathic peptides with hydrophilic and hydrophobic parts in the two opposite ends (a highly hydrophilic N terminus and a mainly hydrophobic C terminus) were reported to have cellular uptake ability.[4] Most CPPs have such an arrangement of the amino acids. On the other hand, secondary amphipathic peptides with the polar residues placed on one face of the helix and the hydrophobic side chains pointing to the opposite face have been reported to have better interaction with the cell membrane.[5]

Positively charged amphipathic peptides are well-suited for interactions with negatively charged biomolecules, such as siRNA. They are short-chain peptides usually containing 20−30 amino acids and are rich in lysine and arginine residues. The interactions between these carriers and their cargo have been reported to involve a combination of hydrophobic and electrostatic contacts through aromatic and charged groups. For example, CADY[6] and PEP family peptides[7] are amphipathic peptides, which have been shown to deliver nucleic acids, peptides, and proteins into a wide variety of cells through the formation of non-covalent complexes. Both the PEP and CADY peptides are rich in tryptophan residues, which appear to play a major role in the stabilization of the carrier/

Received: February 1, 2013
Revised: April 23, 2013
Published: April 24, 2013

cargo complex and insertion into the membrane, owing to their hydrophobic nature. The helical conformation of these peptides, associated with their amphipathic character, has been reported to be essential for their interaction with the cell membrane and their overall function as a CPP.[8]

In biological systems, many types of supramolecular assemblies of proteins play pivotal roles. Many proteins assemble by interactions between secondary structures, such as α-helices and β-sheets, to form large aggregates or assemblies. For example, interactions between α-helices result in capsule-like protein assemblies, such as ferritin[9] and clathrins.[10] The internal skeleton of tomato bushy stunt virus is built by the formation of intermolecular β-sheets among C3 symmetric protein units.[11] Chen et al. have employed different self-assembly mechanisms to develop peptides for hydrophobic drug delivery purposes.[12] In the current work, peptide self-assembly was employed to facilitate the formation of peptide layers to stabilize the siRNA−peptide complex and protect it against degradation.

The design of peptides as carriers for delivery of nucleic acids must take into account the stability of the complex, its ability to penetrate, and most crucially, the release of the cargo inside the cell. Both lysine- and arginine-based peptides have been used for efficient packaging of DNA into nanoparticles to prevent cellular degradation and improve DNA availability. However, it was reported that lysine-containing peptides show differential release of DNA *in vitro* compared to arginine-containing peptides.[13] On the other hand, the guanidine moiety in arginine was reported to play a crucial role in the interaction of the peptide with the cell membrane and its internalization, because replacing arginine with lysine residues that have the same net charge significantly reduced the peptide uptake.[14]

In a previous work, we introduced and characterized the C6 peptide as a siRNA delivery carrier.[15] Three types of amino acids were included in the design of the C6 peptide (Figure 1): (i) 10 leucine residues to induce helicity and amphiphilicity in the peptide structure, (ii) 7 arginine residues to interact with cell membrane components and siRNA molecules, and (iii) an aromatic tryptophan residue as an intrinsic fluorescence probe. The current work introduces the C6M1 peptide, a modified version of C6. As shown in Figure 1, three leucine residues in C6, i.e., Leu3, Leu7, and Leu14, were replaced by tryptophan residues (C6M1). As mentioned, tryptophan seems to play an important role in the interaction of the peptide with cell membrane components, facilitating the direct internalization or endocytosis. The effect of this modification on the peptide solubility, secondary structure, and internalization efficiency will be discussed.

MATERIALS AND METHODS

Peptides, siRNA, and Chemicals. C6 [molecular weight (M_w) = 2470.2, purity > 98%] and C6M1 (M_w = 2689.4, purity > 98%) were purchased from CanPeptide, Inc. (Pointe-Claire, Quebec, Canada). Unlabeled and Cy3-labeled glyceraldehyde 3-phosphate dehydrogenase (GAPDH) siRNA were purchased from Ambion (Austin, TX). Trifluoroethanol (TFE), anilinonaphthalene sulfonate (ANS), and all other chemicals for buffer preparations were obtained from Sigma-Aldrich (Oakville, Ontario, Canada) and used as received.

Formulation of Peptide−siRNA Complexes. The peptide solution was prepared by dissolving peptide powder in RNase-free water. A stock solution of 1 mM was made and diluted at desirable concentrations for various experiments. The solution was then vortexed for 10 s and sonicated for 10 min in a tabletop ultrasonic cleaner (Branson, model 2510, Danbury, CT). siRNA was diluted in RNase-free water to a concentration of 50 μM. Peptide−siRNA complexes were formed by adding peptide solution into siRNA in a proportion according to the designed experiment. The complexes were incubated for 20 min at room temperature before each experiment.

Fluorescence Spectroscopy. To evaluate the hydrophobicity of C6 and C6M1 peptides, the well-established ANS fluorescence assay was applied. Fresh peptide solutions at different concentrations were mixed with the same volume of the ANS solution (20 μM) on a vortex mixer for 20 s. As a control sample, the ANS solution was also mixed with the same volume of pure water. The ANS fluorescence was acquired on a Photon Technology International spectrofluorometer (type LS-100, London, Ontario, Canada) with a pulsed xenon lamp as the light source. Samples (80 μL) were transferred to a quartz cell (1 × 1 cm) and excited at 360 nm, and the emission spectra were collected at wavelengths from 420 to 670 nm. The spectra were normalized with the average intensity of the control sample (I_s) from 650 to 670 nm.

Circular Dichroism (CD) Spectroscopy. C6 and C6M1 solutions (80 μM) were prepared in water, 50% TFE, or NaCl solutions. Spectra from 250 to 190 nm with spectral resolution and pitch of 1 nm and scan speed of 200 nm/min were recorded with a J-810 spectropolarimeter (Jasco, Easton, MD). Samples were transferred into 1 mm long quartz cells and maintained at 25 °C. Spectra shown are the average of three replicates. The raw CD ellipticity (in millidegrees) was converted to residue molar ellipticity (deg cm^2 dmol^{-1} residue^{-1}): $\theta = \theta_{raw}/(10 \times C \times N \times l)$, where θ_{raw} is the ellipticity in millidegrees, C is the peptide concentration (mol/L), l is the optical path length of the cell (cm), and N is the number of residues. The secondary structure composition of the peptide was estimated from CD spectra using the K2D3 program.[16]

Fourier Transform Infrared (FTIR) Spectroscopy. A Vertex 70 (Bruker Optics, Inc., Billerica, MA) FTIR spectrometer, equipped with a liquid-nitrogen-cooled MCT detector, was used to determine the secondary structure of C6M1 (40 μM) in water and 200 mM NaCl solution. The FTIR spectrum of the sample was recorded at a wavenumber resolution of 4 cm^{-1} between 4000 and 400 cm^{-1} using the OPUS 5.5 software (Bruker Optics, Inc., Billerica, MA). After the baseline was subtracted, the absorption spectrum was analyzed in the range of 1575−1725 cm^{-1}, where the amide I band is located.

Surface Tension Measurement. The dynamic surface tension of fresh C6 and C6M1 solutions (100 μM) and C6M1−siRNA solutions was measured over a period of 1.5 h using the axisymmetric drop shape analysis-profile (ADSA-P) technique. A pendant drop of the sample solution was formed at the tip of a vertical Teflon needle (0.92 mm inner diameter) connected to a motor-driven microsyringe. The sample was placed in a temperature-controlled chamber, saturated with water vapor to maintain consistent humidity. The entire system was placed on a vibration-free table. The images of the pendant drop were magnified by an optical microscope and then captured by a charge-coupled device (CCD) camera at 30 s intervals before being transferred to a computer. Images were analyzed by image processing software to generate a profile of the pendant drop. A theoretical curve governed by the Laplace equation of capillarity was then fitted to the profile, generating

dx.doi.org/10.1021/bi4001326 | *Biochemistry* 2013, 52, 3428−3435

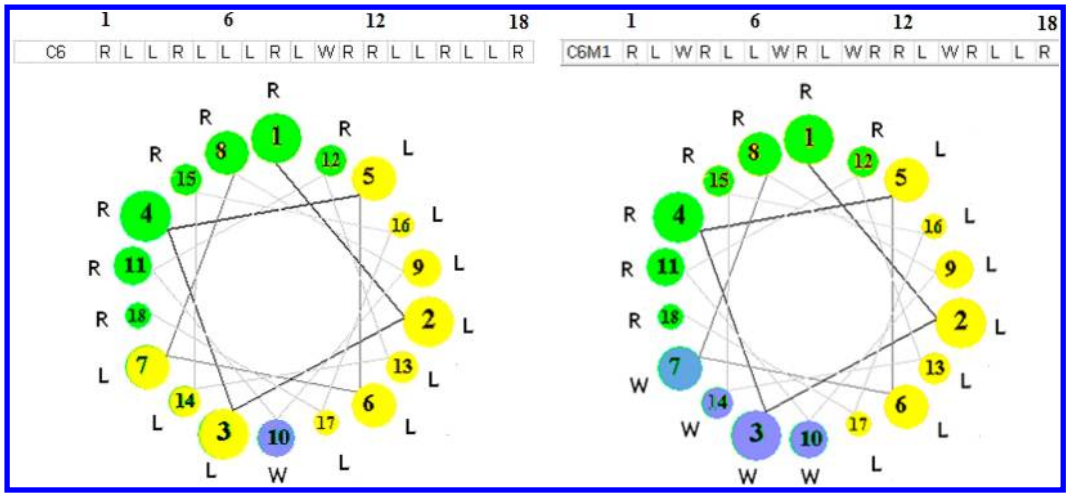

Figure 1. Peptides C6 and C6M1 sequences and helical wheels representation. A downward cross-sectional view of the helix axis is shown for C6 and C6M1. The axis of the α-helix is orthogonal to the paper plane. R, L, and W represent arginine, leucine, and tryptophan residues, respectively.

the surface tension value as a fitting parameter. The maximum standard deviation of the surface tension values was less than 0.3 mN/m.

Cytotoxicity. Chinese hamster ovary (CHO-K1) cells were used for *in vitro* cellular toxicity studies of C6 and C6M1 peptides. Cells were detached from the flasks by adding trypsin−ethylenediaminetetraacetic acid (EDTA) and incubating for 5 min, centrifuged at 500 rpm for 5 min, and resuspended in fresh cell culture media, F-12K containing 10% fetal bovine serum (FBS), at a concentration of 1×10^5 cells/mL. A total of 100 μL of cell suspension was added to each well of a flat bottom, 96-well plate and incubated for 24 h. The media was then replaced with fresh medium with different final concentrations of C6 and C6M1 or controls. The cell counting kit-8 (CCK-8, Dojindo, Japan) was used to perform cytotoxicity assays, 24 h post-treatment. A total of 10 μL of CCK-8 substrate was added to each well without discarding the old media and incubated for an additional 1 h at 37 °C in the dark. Absorbance was measured at a wavelength of 450 nm with a reference wavelength of 620 nm using a microplate reader (FLUOstar OPTIMA, BMG, Cary, NC). The 50% inhibitory concentration (IC_{50}) of peptides on cells was calculated using CCK-8 data.

Flow Cytometry. The amount of intracellular Cy3-labeled siRNA was quantified by flow cytometry (type BD Biosciences, BD FACS Vantage SE Cell Sorter, San Jose, CA). Approximately 50 000 CHO-K1 cells were seeded in a 24-well cell culture plate, 24 h before treatment. Cy3-labeled GAPDH siRNA was complexed with C6 and C6M1 peptides at peptide/siRNA molar ratios (MRs) of 15:1 and 30:1, respectively, and incubated at room temperature for 20 min. The complexes or naked siRNA samples were added to cells at a final siRNA concentration of 50 nM and incubated at 37 °C for 3 h in Opti-MEM (Invitrogen). The medium was then removed by aspiration, and the wells were washed with trypsin [0.5 mg/mL in phosphate-buffered saline (PBS) for 5 min] and heparin (0.5 mg/mL in PBS for 3 × 10 min) to remove surface-bound complexes. After washing, the cells were detached from the plate by adding trypsin−EDTA and resuspended in fresh 4% paraformaldehyde (PFA) in PBS and collected in fluorescence-activated cell sorting (FACS) tubes for analysis.

RESULTS AND DISCUSSION

Design of C6M1 by Sequence Modification of C6. The C6 peptide was previously reported as a designed amphipathic peptide for siRNA delivery.[15] Despite its ability in cellular delivery of siRNA, C6 suffered from relatively poor solubility and aggregation because of its hydrophobic nature. The solubility of a peptide in the medium is an important factor in the assembly of the peptide−siRNA complex. Moreover, the size of the complex determines the membrane penetration mechanism and efficiency.[17]

Figure 1 shows the sequence and helical wheel projection of C6 and C6M1. In the helical wheel presentation, the side chains of residues forming the α-helix are projected onto a circle in a plane perpendicular to the axis of the helix. Assuming the periodicity of an ideal α-helix, there is a 100° angle between consecutive amino acid residues in the wheel diagram. As shown in Figure 1, both peptides were designed to show amphiphilicity by clustering of hydrophilic residues (i.e., arginine) on one side and hydrophobic residues (i.e., leucine and tryptophan) on the opposite side of the circle. C6M1 was originally designed from C6 by replacing leucine residues with tryptophan in 3, 7, and 14 positions. The tryptophan content and distribution were reported to alter the cellular uptake of the CPPs.[18] This modification was also meant to improve the helicity and solubility of the peptide in a polar environment.

The modified 18-mer peptide, C6M1, consists of three types of amino acids, i.e., 7 arginine, 7 leucine, and 4 tryptophan residues. Arginine residues interact with negatively charged cell membrane phospholipids or proteoglycans mainly through guanidine moieties to trigger direct translocation or endocytosis.[19] They also form non-covalent complexes with negatively charged cargos, e.g., siRNA, through electrostatic interaction. Leucine residues interact with hydrophobic tails of the lipid bilayer, facilitating the translocation of the peptide.[1] They are also required for self-assembly of the peptide, which can create external layers to protect the peptide−siRNA core from degradation. The aromatic tryptophan residues have been reported to greatly enhance the cellular uptake of arginine-rich peptides.[8] The design of C6M1 allows for the arrangement of all tryptophan residues at the same face of the helix. This arrangement is also expected to stabilize the helical structure through a $\pi-\pi$ interaction between tryptophan rings.

dx.doi.org/10.1021/bi4001326 | *Biochemistry* 2013, 52, 3428−3435

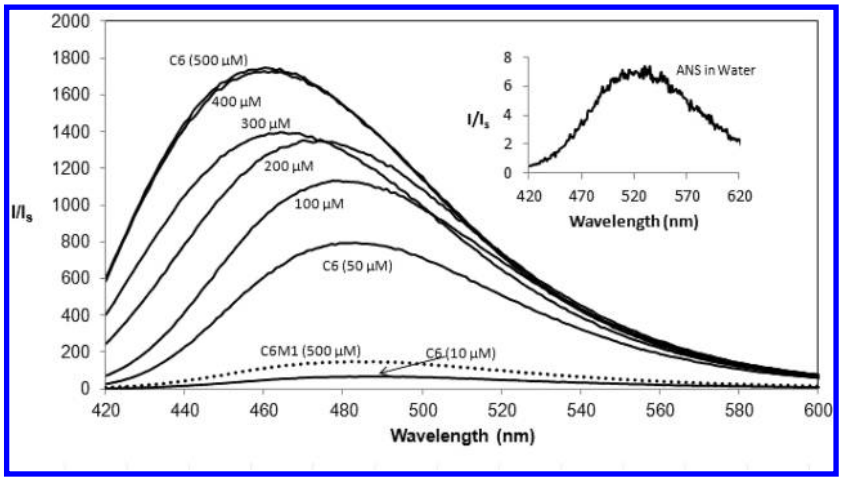

Figure 2. ANS fluorescence of C6 (10−500 μM) and C6M1 (500 μM). The final concentration of ANS was 10 μM. The inset plot shows the fluorescence of ANS in water at the absence of peptides. The fluorescence intensity of all samples was normalized to that of the water sample at 670 nm (I_s).

Effect of Sequence Modification on the Hydrophobicity of the Peptide. ANS is a hydrophobic dye molecule, which binds to hydrophobic areas of folded proteins. Because of the high sensitivity of ANS to the polarity of the environment, it has been widely used as a probe to study the hydrophobicity of the molecules, protein aggregation, and cell membrane composition.[20,21] The fluorescence intensity and peak position of ANS change depending upon its environment. In a low-polar environment, the fluorescence intensity of ANS increases along with a blue shift in the fluorescence spectrum peak toward lower wavelengths.

As shown in Figure 2, the peak positions for ANS fluorescence were different at different solutions; it located at ∼520 nm for water (inset) but shifted to ∼490 and ∼460 nm for C6M1 (500 μM) and C6 (500 μM) solutions, respectively. The normalized ANS fluorescence intensity was also much higher for C6 compared to that of C6M1 at the same concentration. This indicates that the sequence modification in C6M1 has greatly decreased its hydrophobicity and improved its solubility in aqueous solutions. The calculation of hydropathy indexes (HIs) of both peptides by averaging those of all amino acids also confirms the ANS results. The replacement of three leucine residues (HI of +3.8) with three tryptophan residues (HI of −0.9) led to the HI of −0.47 for C6M1 compared to that of C6 (HI of +0.31). The number of arginine residues (HI of −4.5) remained the same in both peptides. Further experiments with C6 showed that the intensity of the fluorescence was concentration-dependent. At higher C6 concentrations, ANS molecules had access to more hydrophobic regions at the surface of C6 aggregates, leading to a more pronounced shift in the peak position along with higher fluorescence intensity, until it reached saturation at concentrations above 400 μM.

The hydrophobicity of the drug/gene carrier is an important factor because it can affect the drug−carrier complex formation, biodistribution, and bioavailability and limit the solubility of the complex in aqueous solutions.

Kinetics of Adsorption of C6 and C6M1 at the Air−Water Interface. Considering the amphipathic feature of C6 and C6M1, the ADSA-P technique was employed to measure the kinetics of adsorption of the peptide at the air−water interface. Figure 3 shows the change in surface tension of C6 and C6M1 solutions (100 μM) over time. The surface tension

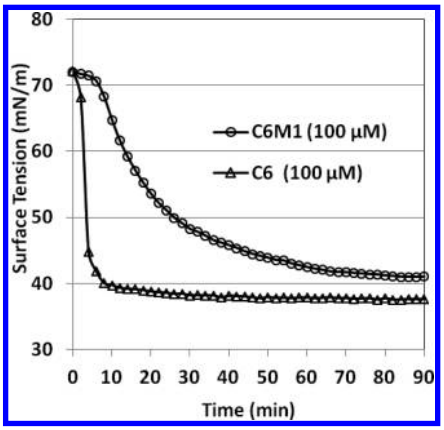

Figure 3. Dynamic surface tension of C6 and C6M1 solutions at a concentration of 100 μM.

of C6 solution dropped fast initially and reached equilibrium after ∼30 min. This indicates fast adsorption of C6 molecules and assemblies at the air−water interface. In contrast, the surface tension of C6M1 solution showed no significant decrease at the first ∼5 min, followed by a gradual decrease to reach equilibrium in ∼90 min. The two different patterns of dynamic surface tension of C6 and C6M1 solutions correspond to different kinetics of adsorption of peptide molecules or assemblies at the air−water interface. Because of the more hydrophobic leucine residues, C6 molecules and aggregates diffuse very quickly from the bulk to the liquid−air interface to minimize the exposure of hydrophobic residues/regions to the aqueous environment, affecting the surface free energy and decreasing the surface tension. However, the sequence modification in C6M1 enables the assembly of the peptide in the bulk and gradual absorption of peptide molecules and assemblies at the interface, resulting in the slower decrease in the surface tension of the solution. The lower equilibrium surface tension of C6 (∼37 mN/m) compared to that of C6M1 (∼41 mN/m) may also reflect the more hydrophobic nature of C6 in comparison to C6M1, confirming the results of the ANS fluorescence assay.

Effect of Complex Composition on the Adsorption of C6M1 at the Air−Water Interface. The surface activity of C6M1 and its complex with siRNA at different MRs was further

dx.doi.org/10.1021/bi4001326 | *Biochemistry* 2013, 52, 3428−3435

studied using the ADSA-P technique. The concentration dependence aggregation/assembly of amphipathic peptides is expected to be analogous to that of surfactants, which have both hydrophilic and hydrophobic moieties. The peptide-induced reduction in surface tension was measured as a function of the peptide bulk concentration. The critical aggregation concentration (CAC) is defined as the concentration for which no further change in surface tension was detected. This was shown as the intersection of a diagonal line fitted to low-concentration data and a horizontal line fitted to high-concentration data, for which the surface tension values were almost constant (Figure 4A). The CAC of C6M1, i.e., ~30 μM, was lower than CACs reported for other amino acid pairing (AAP) peptides (~60 μM for EAK-16-II).[22,23] However, the reduction in surface tension at CAC (~30 mN/m) was much higher than those of other reported AAP peptides (~10 mN/m for EAK-16-II), which reflected the stronger surface activity of C6M1.

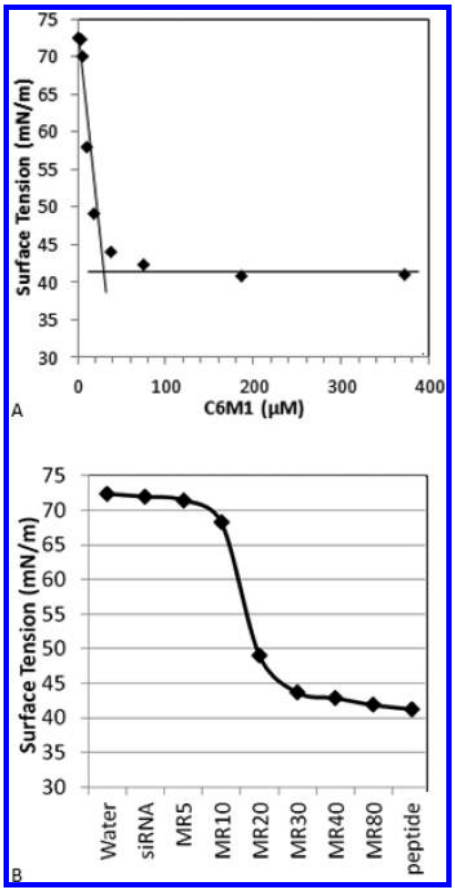

Figure 4. (A) Equilibrium surface tension of C6M1 solution as a function of the peptide concentration. The intersection of two fitted lines indicates the CAC of C6M1 (~30 μM). (B) Surface tension of solutions containing C6M1–siRNA complexes at a fixed peptide concentration of 100 μM and different MRs.

The adsorption property of C6M1 was changed by its interaction with siRNA. Peptide–siRNA complexes at MRs from 0 to 80:1 were obtained using a fixed peptide concentration of 100 μM and varying the siRNA concentration. As shown in Figure 4B, the surface tension of siRNA solution (20 μM) was the same as that of water, indicating that siRNA did not have a surface-active nature. At low MRs up to 10:1, the siRNA molecules were enough to interact with whole C6M1 molecules, which could eventually trap them in the bulk, resulting in no change in surface tension of the solution. However, at higher MRs, e.g., 80:1, the excess of C6M1 molecules could create extra layers on the already formed peptide–siRNA complex core through AAP peptide–peptide interactions. The presence of C6M1 molecules on the surface of the complex could regain the ability of the complex to be absorbed in the air–water interface, resulting in the same drop in surface tension as that of free peptide, i.e., ~30 mN/m. According to Figure 4B, a MR of at least 20:1 was required to gain surface-active properties. The surface activity of the complex is required to efficiently interact with the cell membrane component and internalize the cells.

Effect of Sequence Modification on the Secondary Structure of the Peptide. The secondary structure of C6 and C6M1 was characterized in water and a membrane-mimicking environment (50% TFE), using CD spectroscopy. As shown in Figure 5A, C6 in water showed a mostly random-coil structure with only ~9% helical content (Table 1). However, C6M1 in water partially (~37%) adopted a helical structure. This increased helicity might be associated with more tryptophan residues in C6M1, which can stabilize the helical structure through π–π stacking of aromatic rings.[24] Both peptides showed a significant increase in helical content in 50% TFE solution (Figure 5A). The secondary structure of C6 and C6M1 in 50% TFE solution included 80 and 93% α-helices, respectively, implying that both peptides adopt mainly helical conformation upon interaction with the cell membrane. TFE

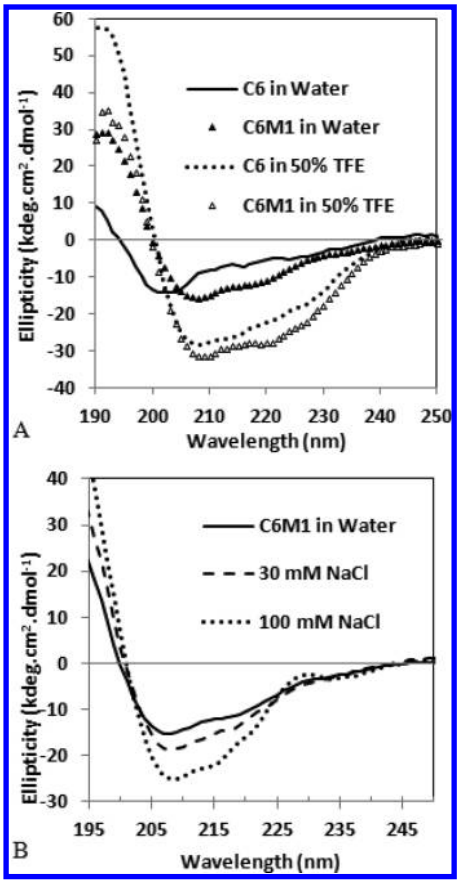

Figure 5. (A) CD spectra of C6 (80 μM) and C6M1 (80 μM) in water and in 50% TFE. (B) CD spectra of C6M1 (80 μM) in water, 30 mM and 100 mM NaCl.

dx.doi.org/10.1021/bi4001326 | *Biochemistry* 2013, 52, 3428–3435

Table 1. Secondary Structure Composition of C6 and C6M1 at Different Conditions

sample	α-helix (%)	random coil (%)	other (%)
C6 in water	9	57	34
C6 in 50% TFE	80	20	0
C6M1 in water	37	45	18
C6M1 in 50% TFE	93	7	0
C6M1 in 30 mM NaCl	40	44	16
C6M1 in 100 mM NaCl	50	38	12

provides a membrane-mimicking environment and has been reported to have a similar effect on CPP secondary structure as phospholipids.[25] By changing its conformation, the peptide attains a more stable structure, which allows for better interaction with cell membranes and enhances cell penetration.[26] Further experiments with C6M1 showed that increasing the ionic strength of the media also increases the helical contents of C6M1 (Figure 5B). Changing the media from water to 30 and 100 mM NaCl solutions led to 40 and 50% helical contents in secondary structure of C6M1, respectively (Table 1). The presence of anionic components in media can screen the positive charge of arginine residues in one face of the helical structure, resulting in a decrease in their charge repulsion and adopting a stable helical structure.

This finding was further confirmed by FTIR spectroscopy. Figure 6 shows the FTIR spectra of C6M1 in the wavenumber

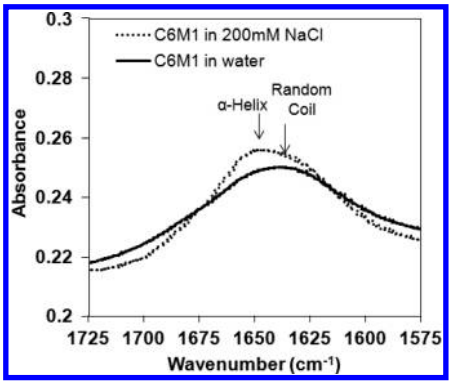

Figure 6. FTIR spectra (amide I region) of C6M1 in water or 200 mM NaCl solution.

range of 1575−1725 cm^{-1}, which corresponds to the amide I band. At this band, the peak of ~1650 cm^{-1} is attributed to the formation of α-helices, whereas random-coil structures occur at 1640 cm^{-1}. The peaks of ~1630 and ~1690 cm^{-1} represent β-sheet structures. As shown in Figure 6, C6M1 in water showed the peak around 1640 cm^{-1}, with a wide shoulder around 1650 cm^{-1}, indicating the presence of a combination of random-coil and α-helical structures. On the other hand, C6M1 in 200 mM NaCl solution adopted mainly α-helical structure (main peak at 1650 cm^{-1}), with a shoulder at 1640 cm^{-1} (random coil). These results are in full agreement with those obtained by CD spectroscopy (Figure 5 and Table 1).

Cytotoxicity of C6 and C6M1 Peptides. To evaluate the cellular toxicity of C6 and C6M1 peptides and whether the modification of C6 peptide could alter its cytotoxicity behavior, a dose−response toxicity assay of both peptides at final concentrations, ranging from 0.1 to 100 μg/mL, was performed on A549 cells. As reported in Figure 7A, peptide C6M1 showed lower toxicity, with an IC_{50} (the concentration of peptide at

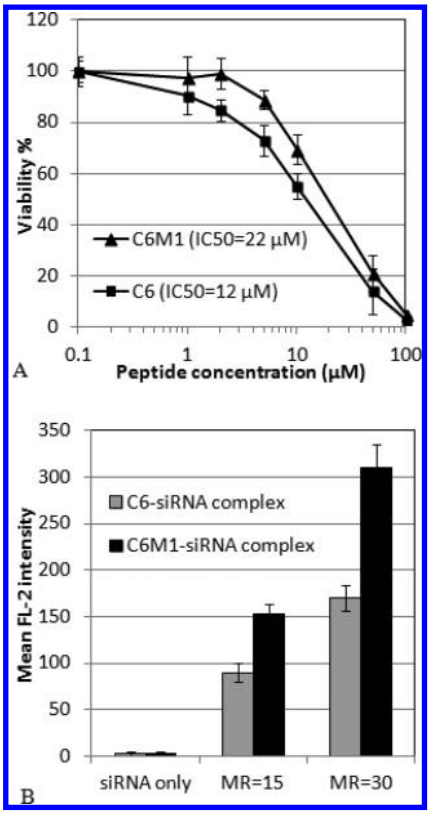

Figure 7. (A) Effect of C6 and C6M1 peptides on the viability of CHO-K1 cells. Cells were cultivated in F-12K medium with indicated concentrations of peptides for 24 h before the toxicity assay. (B) Uptake of Cy3-labeled siRNA alone or in complex with C6 and C6M1 peptides at peptide/siRNA MRs of 15:1 and 30:1. Fluorescence values were normalized to that of non-treated cells (uptake = 0%). Error bars represent the standard deviation of three independent experiments in both panels.

50% cell viability) of 22 μM, compared to C6 with an IC_{50} of 12 μM. This shows that modification of peptide C6 by replacing three leucine residues with less hydrophobic tryptophan residues significantly reduced its cytotoxicity. Peptide C6 has shown high membrane perturbing activity and pore formation tendency, leading to cytotoxicity at a high concentration above 2 μM (not published). However, the modification of the peptide sequence in C6M1 reduced toxic properties, making this peptide a safer carrier at concentrations used for siRNA delivery (below 4 μM).

Effect of Sequence Modification on the Peptide Uptake Efficiency. The efficiency of C6 and C6M1 peptides in delivering labeled Cy3−siRNA was evaluated by flow cytometry. This technique determines the quantity of intracellular complexes by measuring the Cy3 fluorescence intensity. Because of the high tendency of these peptides to attach to the cell membrane surface, a trypsin/heparin washing procedure was employed to ensure detachment of surface-bound complexes. After treatment with C6−siRNA or C6M1−siRNA complexes for 2 h at 37 °C, cells were washed with PBS, trypsin (0.5 mg/mL in PBS for 5 min), and heparin (0.5 mg/mL in PBS for 3 × 10 min), before flow cytometry analysis.

As shown in Figure 7B, siRNA by itself was unable to cross the cell membrane; however, the complex of siRNA with C6 or C6M1 showed significant uptake in CHO-K1 cells, which was dependent upon the MR of peptide/siRNA. Replacing three leucine residues (C6) with tryptophan residues (C6M1) led to

dx.doi.org/10.1021/bi4001326 | Biochemistry 2013, 52, 3428−3435

a ~90% increase in uptake efficiency of the peptide at both MRs, implying the role of tryptophan residues in facilitating the uptake of the complex. In a similar study, Bechara et al. reported the unique role of tryptophan residues in the interaction of cationic CPPs with cell surface glycosaminoglycans (GAGs), facilitating direct penetration or GAG-dependent endocytosis.[27] It is worth noting that the uptake efficiency of the peptide−siRNA complex does not necessarily reflect its transfection efficiency, because some complexes may trap in endosomes or have difficulties in releasing siRNA in the case of aggregation.

■ CONCLUSION

In this study, a new amphipathic peptide, C6M1, a modified version of the already-reported C6 peptide, was introduced as a safer and more efficient carrier for siRNA delivery. The impact of the replacement of three leucine residues with tryptophan residues in the peptide sequence on its solubility, secondary structure, cytotoxicity, and uptake efficiency was investigated. ANS fluorescence and surface tension experiments showed that the sequence modification significantly enhanced the solubility of the peptide in aqueous solution. C6M1 also showed more helical content in its secondary structure compared to C6 in water, saline, and 50% TFE solutions. This modification significantly reduced the cytotoxity of the peptide, making it a safer carrier for siRNA delivery. C6M1 was also found ~90% more efficient than C6 in delivering Cy3-labeled siRNA in CHO-K1 cells.

■ AUTHOR INFORMATION

Corresponding Author

*Telephone: +1-519-888-4567, ext. 35586. Fax: 1-519-888-4347. E-mail: p4chen@uwaterloo.ca.

Funding

This research was financially supported by the Natural Sciences and Engineering Research Council of Canada (NSERC), the Canada Research Chairs (CRC) Program, and the Waterloo Institute for Nanotechnology (WIN) fellowship to Mousa Jafari.

Notes

The authors declare no competing financial interest.

■ ACKNOWLEDGMENTS

We thank Ran Pan and Kaveh Sarikhani for their assistance in cell culture and surface tension experiments, respectively.

■ ABBREVIATIONS USED

AAP, amino acid pairing; ADSA-P, axisymmetric drop shape analysis-profile; ANS, anilinonaphthalene-8-sulfonic acid; CAC, critical aggregation concentration; CCK, cell counting kit; CD, circular dichroism; CHO, Chinese hamester ovary; CPP, cell-penetrating peptide; EDTA, ethylenediaminetetraacetic acid; FACS, fluorescence-activated cell sorting; FBS, fetal bovine serum; GAG, glycosaminoglycan; GAPDH, glyceraldehyde 3-phosphate dehydrogenase; HI, hydropathy index; MR, molar ratio; M_w, molecular weight; PBS, phosphate-buffered saline; siRNA, short interfering RNA

■ REFERENCES

(1) Langel, Ü. *Handbook of Cell-Penetrating Peptides*, 2nd ed.; CRC Press (Taylor and Francis Group): Boca Raton, FL, 2007.

(2) Säälik, P., Elmquist, A., Hansen, M., Padari, K., Saar, K., Viht, K., Langel, Ü., and Pooga, M. (2004) Protein cargo delivery properties of cell-penetrating peptides. A comparative study. *Bioconjugate Chem. 15*, 1246−1253.

(3) Zorko, M., and Langel, Ü. (2005) Cell-penetrating peptides: Mechanism and kinetics of cargo delivery. *Adv. Drug Delivery Rev. 57*, 529−545.

(4) Deshayes, S., Plenat, T., Aldrian-Herrada, G., Divita, G., Grimmellec, C. D., and Heitz, F. (2004) Primary amphipathic cell-penetrating peptides: Structural requirements and interactions with model membranes. *Biochemistry 43*, 7698−7706.

(5) Ohmori, N., Niidome, T., Kiyota, T., Lee, S., Sugihara, G., Wada, A., Hirayama, T., and Aoyagi, H. (1998) Importance of hydrophobic region in amphiphilic structures of α-helical peptides for their gene transfer-ability into cells. *Biochem. Biophys. Res. Commun. 245*, 259−65.

(6) Tros de Ilarduya, C., Sun, Y., and Düzgüneş, N. (2010) Gene delivery by lipoplexes and polyplexes. *Eur. J. Pharm. Sci. 40*, 159−170.

(7) Deshayes, S., Morris, M., Heitz, F., and Divita, G. (2008) Delivery of proteins and nucleic acids using a non-covalent peptide-based strategy. *Adv. Drug Delivery Rev. 60*, 537−547.

(8) Kurzawa, L., Pellerano, M., and Morris, M. C. (2010) PEP and CADY-mediated delivery of fluorescent peptides and proteins into living cells. *Biochim. Biophys. Acta 1798*, 2274−2285.

(9) Lawson, D. M., Artymiuk, P. J., Yewdall, S. J., Smith, J. M., Livingstone, J. C., Treffry, A., Luzzago, A., Levi, S., Arosio, P., and Cesareni, G. (1991) Solving the structure of human H ferritin by genetically engineering intermolecular crystal contacts. *Nature 349*, 541−544.

(10) Fotin, A., Cheng, Y., Grigorieff, N., Walz, T., Harrison, S. C., and Kirchhausen, T. (2004) Structure of an auxilin-bound clathrin coat and its implications for the mechanism of uncoating. *Nature 432*, 649−653.

(11) Olson, A. J., Bricogne, G., and Harrison, S. C. (1983) Structure of tomato busy stunt virus IV. the virus particle at 2.9 Å resolution. *J. Mol. Biol. 171*, 61−93.

(12) Fung, S., Yong, H., Sadatmousavi, P., Sheng, Y., Mamo, T., Nazaian, R., and Chen, P. (2011) Amino acid pairing for de novo design of self-assembling peptides and their drug delivery potential. *Adv. Funct. Mater. 21*, 2456−2464.

(13) Mann, A., Thakur, G., Shukla, V., Singh, A. K., Khanduri, R., Naik, R., Jiang, Y., Kalra, N., Dwarakanath, B. S., Langel, Ü., and Ganguli, M. (2011) Differences in DNA condensation and release by lysine and arginine homopeptides govern their DNA delivery efficiencies. *Mol. Pharm. 8*, 1729−1741.

(14) Wender, P. A., Mitchell, D. J., Pattabiraman, K., Pelkey, E. T., Steinman, L., and Rothbard, J. B. (2000) The design, synthesis, and evaluation of molecules that enable or enhance cellular uptake: Peptoid molecular transporters. *Proc. Natl. Acad. Sci. U.S.A. 97*, 13003−13008.

(15) Jafari, M., Xu, W., Naahidi, S., Chen, B., and Chen, P. (2012) A new amphipathic, amino-acid-pairing (AAP) peptide as siRNA delivery carrier: Physicochemical characterization and in vitro uptake. *J. Phys. Chem. B 116*, 13183−13191.

(16) Louis-Jeune, C., Andrade-Navarro, M. A., and Perez-Iratxeta, C. (2012) Prediction of protein secondary structure from circular dichroism using theoretically derived spectra. *Proteins: Struct., Funct., Bioinf. 80*, 374−381.

(17) Gratton, S. E., Ropp, P. A., Pohlhaus, P. D., Luft, J. C., Madden, V. J., Napier, M. E., and DeSimone, J. M. (2008) The effect of particle design on cellular internalization pathways. *Proc. Natl. Acad. Sci. U.S.A. 105*, 11613−11618.

(18) Rydberg, H. A., Matson, M., Amand, H. L., Esbjorner, E. K., and Norden, B. (2012) Effects of tryptophan content and backbone spacing on the uptake efficiency of cell-penetrating peptides. *Biochemistry 51*, 5531−5539.

(19) Nakase, I., Tadokoro, A., Kawabata, N., Takeuchi, T., Katoh, H., Hiramoto, K., Negishi, M., Nomizu, M., Sugiura, Y., and Futaki, S. (2007) Interaction of arginine-rich peptides with membrane-associated proteoglycans is crucial for induction of actin organization and macropinocytosis. *Biochemistry 46*, 492−501.

(20) Eastoe, J., and Dalton, J. S. (2000) Dynamic surface tension and adsorption mechanisms of surfactants at the air−water interface. *Adv. Colloid Interface Sci. 85*, 103−144.
(21) Matulis, D., Baumann, C. G., Bloomfield, V. A., and Lovrien, R. E. (1999) 1-Anilino-8-naphthalene sulfonate as a protein conformational tightening agent. *Biopolymers 49*, 451−458.
(22) Fung, S. Y., Keyes, C., Duhamel, J., and Chen, P. (2003) Concentration effect on the aggregation of a self-assembling oligopeptide. *Biophys. J. 85*, 537−548.
(23) Fung, S. Y., Yang, H., and Chen, P. (2008) Sequence effect of self-assembling peptides on the complexation and in vitro delivery of the hydrophobic anticancer drug ellipticine. *PLoS One 3*, No. e1956.
(24) Danylyuk, O., and Fedin, V. (2012) Solid-state supramolecular assemblies of tryptophan and tryptamine with cucurbit[6]uril. *Cryst. Growth Des. 12*, 550−555.
(25) Houston, M. E., Kondejewski, L. H., Karunaratne, D. N., Gough, M., Fidai, S., Hodges, R. S., and Hancock, R. E. (1998) Influence of preformed α-helix and α-helix induction on the activity of cationic antimicrobial peptides. *J. Peptide Res. 52*, 81−88.
(26) Sani, M. A., Whitwell, T. C., and Separovic, F. (2012) Lipid composition regulates the conformation and insertion of the antimicrobial peptide maculatin 1.1. *Biochim. Biophys. Acta 1818*, 205−211.
(27) Bechara, C., Pallerla, M., Zaltsman, Y., Burlina, F., Alves, I. D., Lequin, O., and Sagan, S. (2012) Tryptophan within basic peptide sequences triggers glycosaminoglycan-dependent endocytosis. *FASEB J. 27*, 738−749.